Jurnal Pharmascience, Volume 13, Issue 1, March 2026, page: 290-308
ISSN-Print 2355 – 5386
ISSN-Online 2460-9560
https://dx.doi.org/10.20527/jps.v13i1.24836
Research Article

# Molecular Docking Studies and ADME-Tox Prediction of Phytocompounds from *Lycopersicon esculentum* mill. as a Drug Candidate for Alopecia Treatment

# *Studi Docking Molekuler dan Prediksi ADME-Tox Senyawa Fitokimia dari Lycopersicon esculentum mill. sebagai Kandidat Obat untuk Pengobatan Alopecia*

Zulpakor Oktoba[1]*, Recky Patala[2], Muhammad Fitra Wardhana Sayoeti[1], Putu Ristyaning Ayu Sangging[3], Tri Umiana Soleha[4]

[1]Pharmacy Department, Faculty of Medicine, Lampung University, Bandar Lampung, Lampung, Indonesia
[2]Pharmacy Department, Faculty of Mathematics and Natural Sciences, Tadulako University, Palu, Central Sulawesi, Indonesia
[3]Clinical Pathology Department, Faculty of Medicine, Lampung University, Bandar Lampung, Lampung, Indonesia
[4]Microbiology and Parasitology Department, Faculty of Medicine, Lampung University, Bandar Lampung, Lampung, Indonesia
Email: zulpakor.oktoba@fk.unila.ac.id

## ABSTRACT

**Alopecia is a disorder of the hair follicles that causes hair loss, either in limited areas or throughout the entire body. This study aims to evaluate the potential and molecular interactions of compounds found in the Rampai plant (*Lycopersicon esculentum* Mill.). The Rampai plant is known to contain various secondary metabolites such as alkaloids, flavonoids, arbutin, amygdalin, and pectin, which have the potential to be developed as antialopecia drug candidates through an in-silico approach to androgen receptors (PDB ID: 4K7A) and ADME-Tox profile predictions. The *in-silico* approach was conducted using the molecular docking method to predict the interaction between the active compounds from the Rampai plant and the androgen receptor using Autodock Tools 1.5.7 and Vina software, while the ADME-Tox analysis was conducted through the pkCSM platform. The molecular docking results showed that the reference ligand (Minoxidil) had an affinity energy of −7.353 kcal/mol, while the test compound with the best affinity was isorhamnetin with a value of −8.398 kcal/mol, which was lower (more**

**stable) than Minoxidil. In addition, the ADME-Tox prediction results for isorhamnetin show favorable pharmacokinetic characteristics, especially in terms of skin permeability, absorption and distribution. Thus, isorhamnetin has the potential as an androgen receptor antagonist and a role in the development of therapies for alopecia.**

**Keywords: ADME-Tox, Alopecia, *In Silico*, *Lycopersicon esculentum*, Receptor Androgen**

***ABSTRAK***

***Alopecia adalah gangguan pada folikel rambut yang menyebabkan kerontokan rambut, baik pada area terbatas maupun di seluruh tubuh. Studi ini bertujuan untuk mengevaluasi potensi dan interaksi molekuler senyawa yang terdapat pada tanaman Rampai (Lycopersicon esculentum Mill.). Tanaman Rampai diketahui mengandung berbagai metabolit sekunder seperti alkaloid, flavonoid, arbutin, amygdalin, dan pektin, yang berpotensi dikembangkan sebagai kandidat obat antialopecia melalui pendekatan in-silico terhadap reseptor androgen (PDB ID: 4K7A) dan prediksi profil ADME-Tox. Pendekatan in-silico dilakukan menggunakan metode docking molekuler untuk memprediksi interaksi antara senyawa aktif dari tanaman Rampai dan reseptor androgen menggunakan Autodock Tools 1.5.7 dan perangkat lunak Vina, sementara analisis ADME-Tox dilakukan melalui platform pkCSM. Hasil docking molekuler menunjukkan bahwa ligan referensi (Minoxidil) memiliki energi afinitas sebesar −7,353 kkal/mol, sedangkan senyawa uji dengan afinitas terbaik adalah isorhamnetin dengan nilai −8,398 kkal/mol, yang lebih rendah (lebih stabil) dibandingkan Minoxidil. Selain itu, hasil prediksi ADME-Tox untuk isorhamnetin menunjukkan karakteristik farmakokinetik yang menguntungkan, terutama dalam hal permeabilitas kulit, penyerapan, dan distribusi. Oleh karena itu, isorhamnetin memiliki potensi sebagai antagonis reseptor androgen dan peran dalam pengembangan terapi untuk alopecia.***

***Kata Kunci: ADME-Tox, Alopecia, In silico, Lycopersicon esculentum, Receptor Androgen***

## I. INTRODUCTION

Hair loss, clinically known as alopecia, is a disorder involving hair follicles that may affect the scalp or extend to other parts of the body, leading to partial or complete hair loss. Alopecia is influenced by multiple factors, including genetic predisposition, environmental exposure, nutritional status, and hormonal imbalance (Chinelo et al., 2018; Guo & Katta, 2017).

Epidemiological studies have reported that alopecia affects millions of individuals worldwide, particularly adults over the age of 35 (Guo & Katta, 2017). Minoxidil is one of the most commonly prescribed synthetic agents for alopecia treatment due to its inhibitory effect on 5-α-reductase activity. However, long-term use of topical minoxidil has been associated with adverse effects such as hypertrichosis and scalp irritation, in addition to its relatively high cost and limited ability to

fully restore hair growth (Abdurrahman et al., 2022).

Indonesia is rich in medicinal plants traditionally used for hair treatment, including *Lycopersicon esculentum* Mill., locally known as rampai. Ethnobotanical studies have reported the traditional use of rampai leaves by communities in Lampung Province to treat dandruff and stimulate hair growth (Oktoba et al., 2018). An ethanol extract of *Erythrina variegate* that contains polyphenol chemicals, terpenoids, tannins, saponins, and steroids promotes hair development in male rabbits, according to Mustarichie et al., (2017). Additionally, chemicals isolated from *E. variegate* were identified through an in-silico analysis using chemical modeling; these compounds bind Janus kinase 2 (JAK2) and may therefore be useful therapeutic treatments for alopecia (Mustarichie et al., 2017). The ethanol, n-hexane, ethyl acetate, and water fractions of extracts from the wera (*Malvaviscus arboreus* Cav.) leaf were found to promote hair development (Mustarichie et al., 2018). Furthermore, studies by (Mustarichie & Hasanah, 2019). shown that cocoa peel extracts in ethanol and n-hexane also promoted rabbit hair development. The study's non-polar n-hexane fraction verified that the discarded cocoa peel (*Theobroma cacao* L.) contained steroid and terpenoid chemicals.

Oktoba et al., (2019) state that terpenoids, steroids, alkaloids, and flavonoids are among the secondary metabolites present in *L. esculentum* leaves, with eighteen terpenoid derivatives already identified. Terpenoids, flavonoids, and alkaloids were found to be substances with antialopecia action.

Previous in vivo and in silico studies have demonstrated that secondary metabolites from medicinal plants can promote hair growth through androgen receptor inhibition and modulation of signaling pathways associated with follicular development (Mustarichie et al., 2017; Mustarichie et al., 2018; Abdurrahman et al., 2021; Badolati et al., 2018). However, studies investigating the anti-alopecia potential and ADME-Tox profiles of *L. esculentum* compounds remain limited. Therefore, this study aims to evaluate the molecular interactions between phytochemical compounds from rampai leaves and the androgen receptor (PDB ID: 4K7A) using a molecular docking approach, along with pharmacokinetic and toxicity prediction through in-silico analysis.

## II. METHOD

### A. Hardware and Software

The hardware used is a PC with Windows 10 64-bit OS specifications,

AMD A6-7310 APU processor with AMD Radeon R4 Graphic 2.00 GHz, and 6 Gigabyte RAM. Analysis was performed with the following software: Discovery Studio Visualizer, Chem3D 15.0, AutoDock Tools 1.5.7, SwissADME and ADME-Tox pkCSM tools.

**B. Materials**

The materials used include the three-dimensional structure of the androgen receptor downloaded from the Protein Data Bank (PDB) (RCSB PDB - 4K7A: Crystal Structure of the Androgen Receptor Ligand Binding Domain in Complex with Minoxidil) (https://www.rcsb.org) with and the two-dimensional structure of the rampai leaves (*L. esculentum* mill.) plant compound taken from (*PubChem*) (https://pubchem.ncbi.nlm.nih.gov/).

**C. Preparation of Ligand Structure**

The ligands used were 25 compounds (ligands) from *Lycopersicon esculentum* mill leaves obtained from https://www.pubchem.org, then stored in .sdf format, followed by geometry optimization using the MM2 command in chem3D 15.0 and stored in .pdb format.

**D. Preparation Protein Receptor**

The androgen receptor's crystal structure (PDB ID: 4K7A) was provided by https://www.rcsb.org/structure/4K7A with a resolution of 2.44 Å. Molecular docking analysis was conducted to predict the interaction between selected phytochemical compounds from *L. esculentum* leaves and the androgen receptor. The three-dimensional structure of the androgen receptor was obtained from the Protein Data Bank. Water molecules and co-crystallized ligands were removed prior to docking to avoid interference during ligand–receptor interaction analysis.

**E. Validation of Molecular Docking Method**

Since water can create hydrogen bonds with the receptor, it could possibly prevent the ligand from attaching to its receptor, which is why validation was done without water. The validation program was carried out by comparing the ligand's native and redocked structures. Root Mean Square Deviation (RMSD) was used to convey the comparison data analysis. If the RMSD value is less than or equal to 2 Å, the docking procedure is deemed successful. According to (Mardianingrum et al., 2021), a method cannot be accepted if the RMSD value obtained is more than 2 Å.

**F. Lipinski Rule of Five**

Lipinski's rule of five (RO5) was used to predict physicochemical parameters in order to ascertain the test substances' permeability for passive diffusion. By

entering the compound's SMILES code into the SwissADME web tool (http://www.swissadme.ch/index.php) and utilizing the features on that page to predict the physicochemical parameters, the test compound structure was produced (Cahyaningrum et al., 2024).

### G. Molecular Docking Simulation

The molecular docking process is carried out between the receptor and ligand (3D compound structure that has undergone screening) using AutoDock Vina software. The first step is to open the Command Prompt (CMD) application, then run the vina.exe file and browse the folder where the prepared receptor files are stored along with the test compounds and reference ligands. Next, the folder address of the receptor file and the test compounds and reference ligands (native ligands) is copied. The docking process is run by typing the command vina.exe --config grid.txt --out test_ligand, then waiting for the docking process to complete. The docking results are saved in .pdbqt format (Weni et al., 2020).

### H. Prediction of ADME-Tox

The ADME-Tox SAR program from http://biosig.unimelb.edu.au/pkcsm/prediction. Using PubChem, the resultant compound's structure was converted to a grin format.

## III. RESULTS AND DISCUSSION

### A. Preparation of Minoxidil Ligand with Test Ligand

The test ligand structures of 25 compounds were derived from rampai leaves (*L. esculentum* mill.) and the native ligand minoxidil, as shown in Table I.

**Table I.** Results of the 2D structure of minoxidil ligand with test ligand

| No | Ligand Name | Structure |
|---|---|---|
| 1 | (+)-β-Phellandrene | 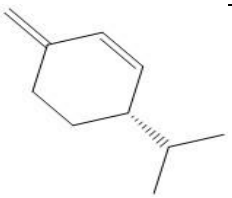 |
| 2 | 2-Carene | 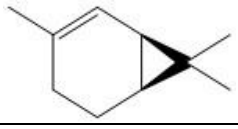 |
| 3 | 2-Hexenal |  |

| No | Ligand Name | Structure |
|---|---|---|
| 4 | α-Pinene | 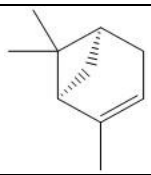 |
| 5 | β-Caryophyllene | 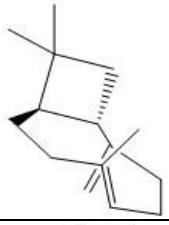 |
| 6 | β-Pinene | 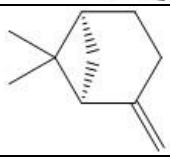 |
| 7 | Caffeic Acid | 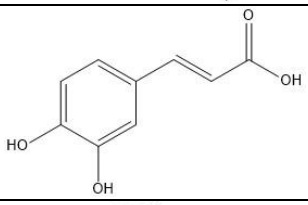 |
| 8 | Camphene |  |
| 9 | Chlorogenic Acid | 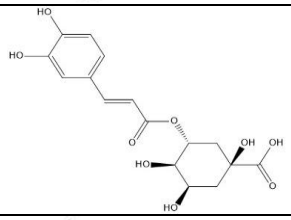 |
| 10 | Eucalyptol | 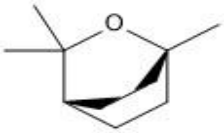 |
| 11 | Eugenol | 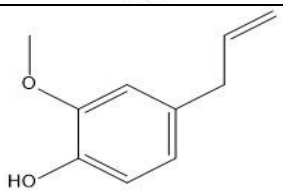 |
| 12 | Ferulic acid | 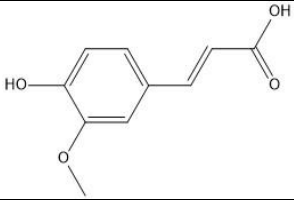 |
| 13 | Gamma Terpinene | 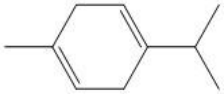 |
| 14 | Hexanal |  |

| No | Ligand Name | Structure |
|---|---|---|
| 15 | Humulene | 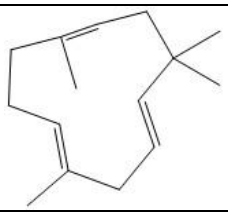 |
| 16 | Isorhamnetin | 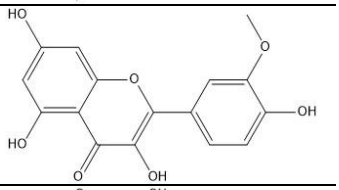 |
| 17 | Kaempferol | 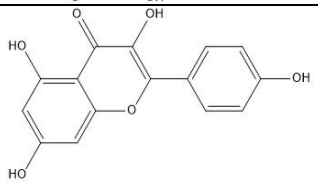 |
| 18 | Limonene | 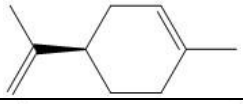 |
| 19 | Linalool | 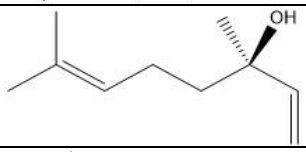 |
| 20 | M-Cymene | 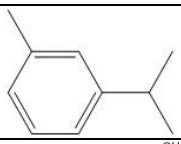 |
| 21 | Myricetin | 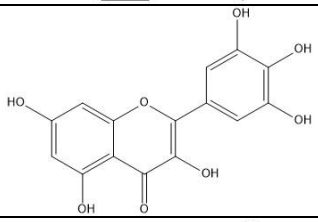 |
| 22 | p-Coumaric Acid | 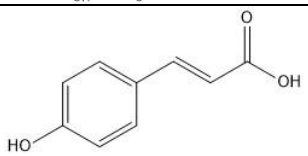 |
| 23 | Quercetin | 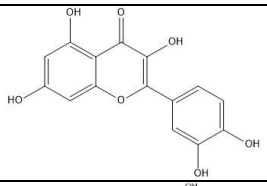 |
| 24 | Rutin | 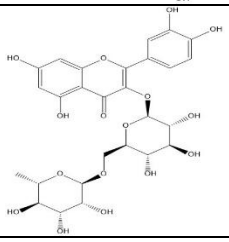 |

| No | Ligand Name | Structure |
|---|---|---|
| 25 | Tomatine | 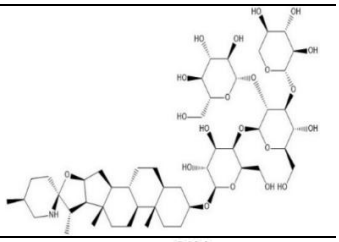 |
| 26 | Minoxidil | 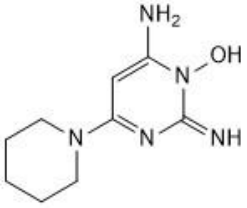 |

**Tabel II**. Predicted physicochemical properties of secondary metabolites in rampai leaves compounds based on Lipinski's Rules

| No. | Compound Name | Molecular Weight (<500 Da) | Log P (<5) | Hydrogen Bond | |
|---|---|---|---|---|---|
| | | | | Donor (<5) | Acceptor (<10) |
| 1 | Isorhamnetin | 316.26 | 1.65 | 4 | 7 |
| 2 | Tomatine | 1034.2 | -0.70 | 13 | 22 |
| 3 | Quercetin | 302.23 | 1.23 | 5 | 7 |
| 4 | Humulene | 204.35 | 4.26 | 0 | 0 |
| 5 | Kaempferol | 286.24 | 1.58 | 4 | 6 |
| 6 | β-Caryophyllene | 204.35 | 4.24 | 0 | 0 |
| 7 | Myricetin | 318.23 | 0.79 | 6 | 8 |
| 8 | Chlorogenic Acid | 354.31 | -0.39 | 6 | 9 |
| 9 | Rutin | 610.5 | -1.51 | 10 | 16 |
| 10 | 2-Carene | 136.23 | 3.12 | 0 | 0 |
| 11 | (+)-β -Phellandrene | 136.23 | 3.07 | 0 | 0 |
| 12 | M-Cymene | 134.22 | 3.58 | 0 | 0 |
| 13 | p-Coumaric Acid | 164.16 | 1.26 | 2 | 3 |
| 14 | Caffeic Acid | 180.16 | 0.93 | 3 | 4 |
| 15 | Eugenol | 164.20 | 2.25 | 1 | 2 |
| 16 | Limonene | 136.23 | 3.37 | 0 | 0 |
| 17 | Gamma-Terpinene | 136.23 | 3.35 | 0 | 0 |
| 18 | Ferulic acid | 194.18 | 1.36 | 2 | 4 |
| 19 | α-Pinene | 136.23 | 3.44 | 0 | 0 |
| 20 | β-Pinene | 136.23 | 3.42 | 0 | 0 |
| 21 | Camphene | 136.23 | 3.43 | 0 | 0 |
| 22 | Eucalyptol | 154.25 | 2.67 | 0 | 1 |
| 23 | Linalool | 154.25 | 2.66 | 1 | 1 |
| 24 | 2-Hexenal | 98.14 | 1.50 | 0 | 1 |
| 25 | Hexanal | 100.16 | 1.66 | 0 | 1 |

In this study, the physicochemical properties of bioactive compounds were assessed using Lipinski's Rule of Five to evaluate their suitability for oral administration. Compounds were considered drug-like if they met the criteria

of molecular weight ≤ 500 Da, logP ≤ 5, fewer than five hydrogen bond donors, and fewer than ten hydrogen bond acceptors (Shofi, 2022). Lipinski RO5 analysis showed that 22 rampai plant compounds met the criteria (Table II). However, tomatine, a steroidal glycoalkaloid with the second-best binding energy, did not comply with RO5 due to its high molecular weight and excessive hydrogen bond donors and acceptors, which may hinder absorption by increasing hydrogen bond formation. Lipinski's rules are used to assess the suitability of active compounds for oral administration. Therefore, compounds that do not meet the criteria in Lipinski's rules are considered unsuitable for formulation as oral preparations (Cahyaningrum et al., 2024).

## B. Preparation of Protein Receptor

Androgen receptors are nuclear hormone receptors that are activated by binding to androgen hormones and function as transcription factors regulating gene expression during male development. In molecular docking studies, these receptors require appropriate ligands to evaluate their interaction potential. The crystal structure of the androgen receptor (PDB ID: 4K7A) was retrieved from the Protein Data Bank with a resolution of 2.44 Å (Figure 1). AutoDock Tools version 1.5.6 was employed to define the grid box and spatial parameters for the docking simulations. The receptor structure was co-crystallized with dihydrotestosterone (DHT) and minoxidil; therefore, the binding position of minoxidil, a known anti-alopecia agent, was used as the reference site for all docking analyses (Abdurrahman et al., 2021).

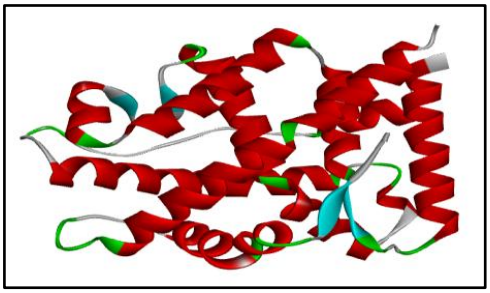

**Figure 1.** 3D structure of the Androgen Receptor macromolecule

## C. Validation of Molecular Docking Method

Docking validation was performed by redocking minoxidil into the androgen receptor (PDB ID: 4K7A) using AutoDock Tools 1.5.7 after removing the native ligands. The grid box was defined based on the original minoxidil binding site, and docking was conducted using predefined grid center (x = 40, y = 40, z = 40) and grid box coordinates (x = 9.416, y = 3.804, z = -7.149 Å). Validation was confirmed by an RMSD value of 0.9571 Å, indicating acceptable accuracy (≤ 2 Å), with hydrogen bond interactions observed at Glu681 and Gln711 (Figures 2 and 3).

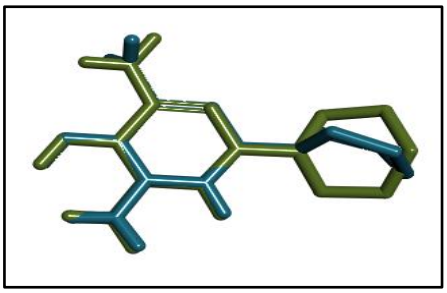

**Figure 2.** Overlay results of crystallized MXD ligand with Redocking ligan

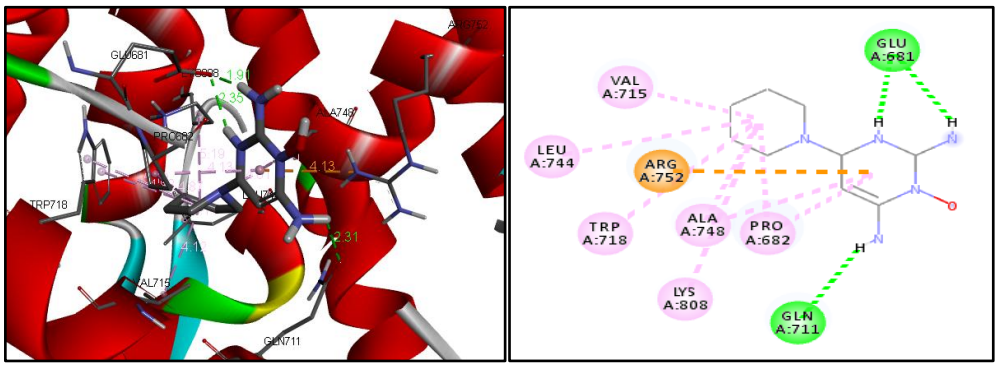


**Figure 3.** The results of MXD ligand redocking to the androgen receptor hydrogen

**Table III**. Molecular Docking Method Validation Results

| PDB ID | Ligand | Bond Energy (kcal/mol) | RMSD (Å) | Hydrogen Bond with Amino Acid | Hydrogen Bond Distance (Å) | Amino Acid Residue |
|---|---|---|---|---|---|---|
| 4K7A | Minoxidil | -7.353 | 0.9571 | Glu681 and Gln711 | 1.91; 2.35 and 2.31 | Val715, Leu744, Trp718, Lys808, Pro682, Ala748 |

**Table IV.** Molecular Docking Results

| Ligand | Bond Energy (kcal/mol) | Hydrogen Bond with Amino Acid | Hydrogen Bond Distance (Å) | Amino Acid Residue |
|---|---|---|---|---|
| Isorhamnetin | -8.398 | Trp751 | 2.59 | Glu681, Leu805, Thr755, Asn756, Val684, Gly683, Val685, Gln711, His714, Val715, Trp718, Lys808. |
| Tomatine | -8.263 | Arg786, Glu793, Gln858 and Lys861 | 2.49; 2.01; 2.92 and 2.57 | Ile869, Leu790, Trp796, Leu797, Leu862, Ser865, His917, Thr918, Lys912. |

| Ligand | Bond Energy (kcal/mol) | Hydrogen Bond with Amino Acid | Hydrogen Bond Distance (Å) | Amino Acid Residue |
|---|---|---|---|---|
| Quercetin | -8.196 | Met745, Leu873 and Leu704 | 2.89; 2.10 and 2.07 | Arg752, Gln711, Leu707, Gly708, Met895, Asn705, Leu701, Phe891, Leu880, Phe876. |
| Humulene | -8.005 | - | - | Thr877, Leu701, Met780, Met787, Val746, Met745, Phe764, Leu707, Gly708, Met895, Trp741. |
| Kaempferol | -7.976 | Val685 | 2.99 | Trp751, Thr755, Glu681, Val684, Gly683, Gln711, His714, Met745, Leu744, Ala748, Pro682. |
| β-Caryophyllene | -7.734 | - | - | Leu707, Val746, Trp741, Gly708, Asn705, Leu704, Met895, Leu873, Thr877. |
| Myricetin | -7.681 | Trp751 and Lys808 | 2.92 and 2.65 | Thr755, Glu681, Leu744, Val715, Gln711, His714, Val685, Gly683, Val684. |
| Chlorogenic Acid | -7.502 | Asn756 | 2.62 | Leu744, Lys808, Glu681, Trp751, Phe804, Thr755, Arg752, Gly683, Val684, Gln711, Met745. |
| Rutin | -7.274 | Glu681, Asn756, Pro682 and Gly683 | 2.57; 2.59; 2.70 and 2.00 | Phe804, Pro801, Glu678, Ala748, Val685, Tyr763, Arg752, Val684. |
| 2-Carene | -7.253 | - | - | Leu744, Trp718, Val715, Lys808, Ala748, Val685, Pro682. |
| (+)-β-Phellandrene | -6.660 | - | - | Gln711, Arg752, Met745, Val715, Leu744, Lys808, Glu681. Val685, Pro682. |

| Ligand | Bond Energy (kcal/mol) | Hydrogen Bond with Amino Acid | Hydrogen Bond Distance (Å) | Amino Acid Residue |
|---|---|---|---|---|
| M-Cymene | -6.616 | - | - | Arg752, Gly683, Leu744, Met745, Lys808, Val715, His714, Gln711, Val685. |
| p-Coumaric Acid | -6.527 | Asn705, Gln711 and Met745 | 2.86; 2.34 and 2.19 | Met895, Leu701, Met780, Leu873, Leu704, Val746, Phe764, Met749 |
| Caffeic Acid | -6.523 | Met745, Gln711 and Arg752 | 2.20; 2.43 and 2.26 | Phe764, Leu707, Gly708, Met895, Asn705, Leu704, Met780, Val746, Met749. |
| Eugenol | -6.519 | Arg752 and Gln711 | 2.56 and 1.90 | Val685, Gly683, His714, Leu744, Lys808, Val715, Trp718, Pro682. |
| Limonene | -6.459 | - | - | Trp718, Glu681, Arg752, Gly683, Gln711, Ala748. |
| Gamma-Terpinene | -6.431 | - | - | Met745, Gln711, Arg752, Val685, His714, Ala748, Val715, Leu744, Lys808, Pro682. |
| Ferulic acid | -6.336 | Lys808, Arg752 and Gln711 | 1.78; 2.39 and 2.74 | Trp718, Leu744, Val715, His714, Gly683, Pro682, Val 685, Val684. |
| α-Pinene | -6.132 | - | - | Met745, Gln711, Ala748, Lys808, Val715, Leu744, Trp718, Pro682, Gly683, Val685, His714. |
| β-Pinene | -6.129 | - | - | Met745. Ala, 748, Trp718, Val715, Pro682. |
| Camphene | -6.116 | - | - | Trp741, Met742, Val746, Arg752, Met749, Gln711, Gly708, Phe764, Leu704. |
| Eucalyptol | -5.971 | - | - | Phe764, Met749, Val746, Leu873, Met745, Trp741, |

| Ligand | Bond Energy (kcal/mol) | Hydrogen Bond with Amino Acid | Hydrogen Bond Distance (Å) | Amino Acid Residue |
|---|---|---|---|---|
| Linalool | -5.748 | - | - | Met895, Gly708, Leu707, Phe764. Gly683, Val684, Glu681, Arg752, Gln711, Met745, His714. |
| 2-Hexenal | -4.603 | - | - | Ala748, Pro682, Leu744, His714, Trp718, Gln711, Val715, Val685, Lys808. |
| Hexanal | -4.500 | Arg752 and Gln711 | 2.30 and 2.95 | Val715, Lys808, Trp718, Pro682, Ala748, Glu681, Leu744, Met745. |

Docking results indicated that isorhamnetin showed a binding free energy of −8.398 kcal/mol (Table IV), which is comparable to that of the reference compound minoxidil −7.353 kcal/mol (Table III), suggesting its potential as an anti-alopecia agent and androgen receptor inhibitor. Minoxidil formed hydrogen bonds with the androgen receptor at residues Glu681 and Gln711, whereas isorhamnetin primarily interacted through a hydrogen bond with Trp751 at a distance of 2.59 Å. The involvement of different amino acid residues, including Leu744 and Lys808, contributed to the lower binding energy of isorhamnetin compared to minoxidil. In addition to hydrogen bonding, hydrophobic interactions were also observed, further stabilizing the ligand–receptor complex, as illustrated in the interaction visualizations (Figures 4 and 5). These interactions occur because nonpolar groups in the protein structure tend to cluster together and avoid contact with water, forming a globular protein structure (Abdurrahman et al., 2022). Complex visualization was performed to identify ligand–receptor interactions, including hydrogen bonds, van der Waals forces, and various hydrophobic interactions. Among these, hydrogen bonding and van der Waals interactions play the most critical roles in stabilizing the ligand–receptor complex (Pantsar & Poso, 2018).

### D. ADME-Toxicity Prediction Results

ADME-Toxicity predictions were performed on three ligand compounds to obtain their pharmacokinetic and toxicological profiles, including absorption, distribution, metabolism, excretion, and toxicity. This testing is very

important to prevent failure in the drug design stage.

Human intestinal absorption (HIA) and Caco-2 permeability were used as indicators of absorption potential. The results showed that isorhamnetin exhibited good intestinal absorption, comparable to minoxidil, while tomatine demonstrated poor absorption characteristics. Skin permeability analysis suggested that isorhamnetin possesses favorable transdermal penetration properties, supporting its potential use in topical alopecia therapy.The HIA value indicates the level of absorption of the active substance in the human intestine, with the following categories: good (70–100%), fair (20–70%), and poor (0–20%). From the analysis results, there are two compounds with good HIA, namely minoxidil and isorhamnetin (Table V).

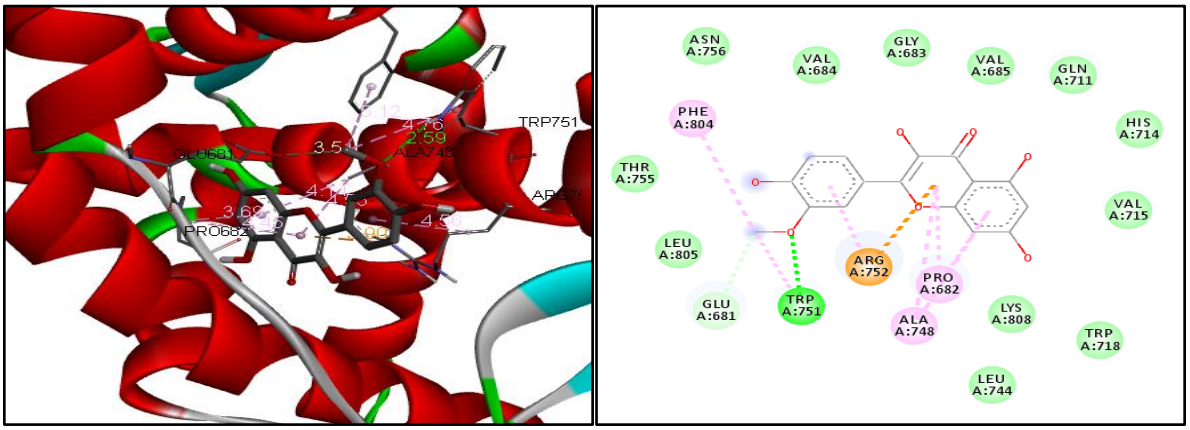


**Figure 4.** Visualization results of the isorhamnetin compound to the androgen receptor

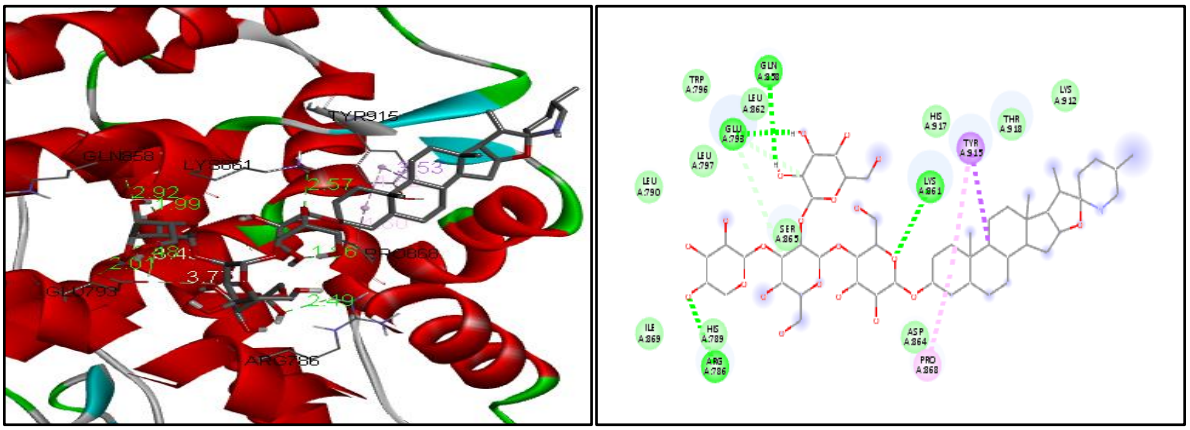


**Figure 5.** Visualization results of the tomatine compound to the androgen receptor

**Table V.** Absorption prediction results

| Compound Name | Absorption | | | |
|---|---|---|---|---|
| | Water solubility ($10^{-3}$ mol/L) | Caco2 permeability (Papp in $10^{-6}$ cm/s) | Intestinal absorption (human) (% Absorbed) | Skin permeability ($10^{-3}$ Kp) |
| Minoxidil | 1.35 | 4.50 | 94.641 | 1.59 |
| Isorhamnetin | 1.00 | 0.993 | 76.014 | 1.84 |
| Tomatine | 1.41 | 0.113 | 0 | 1.84 |

**Table VI.** Distribution prediction results

| Compound Name | Distribution | | | |
|---|---|---|---|---|
| | VDss (human) (L/kg) | Fraction unbound (human) (Fu) | BBB permeability (log BB) | CNS permeability (PS) |
| Minoxidil | 1.39 | 0.773 | -0.951 | $3.38\times10^{-4}$ |
| Isorhamnetin | 13.28 | 0.091 | -1.135 | $6.49\times10^{-4}$ |
| Tomatine | 0.258 | 0.447 | -2.1 | $1.74\times10^{-6}$ |

**Table VII.** Metabolism prediction results

| Compound Name | Metabolism | |
|---|---|---|
| | CYP3A4 substrate (Yes/No) | CYP2C9 inhibitor (Yes/No) |
| Minoxidil | No | No |
| Isorhamnetin | No | No |
| Tomatine | No | No |

**Table VIII.** Excretion prediction results

| Compound Name | Excretion |
|---|---|
| | Total Clearance (mL/min/kg) |
| Minoxidil | 1.88 |
| Isorhamnetin | 3.22 |
| Tomatine | 3.23 |

**Table IX.** Toxicity prediction results

| Compound Name | Toxicity | | | | | | | |
|---|---|---|---|---|---|---|---|---|
| | AMES toxicity (Yes/No) | Maximum tolerated dose (human) (mg/kg/day) | hERG I inhibitor (Yes/No) | hERG II inhibitor (Yes/No) | Oral rat acute toxicity (LD50) (mol/kg) | Hepatotoxicity (Yes/No) | Skin sensitisation (Yes/No) | Minnow toxicity (mM) |
| Minoxidil | No | 0.438 | No | No | 2.286 | Yes | No | 3280 |
| Isorhamnetin | No | 3.77 | No | No | 2.407 | No | No | 161 |
| Tomatine | No | 0.0295 | No | Yes | 2.556 | Yes | No | - |

Caco-2 permeability predictions are used to assess the ability of drugs to penetrate adenocarcinoma epithelial cells in the colon. Permeability categories are classified as low (<4), moderate (4–70), and high (>70). Based on the test results, the two ligands isorhamnetin, and tomatine have low permeability (Table V).

Another parameter analyzed was the blood-brain barrier (BBB), which

describes the ability of a compound to cross the blood-brain barrier. A BBB value > 0.3 indicates that the compound easily crosses the blood-brain barrier, while a value < −1 indicates that the compound is difficult or impossible to penetrate the brain. Based on the analysis results, isorhamnetin and tomatine have the potential to be difficult or impossible to penetrate the blood-brain barrier (Table VI).

Another evaluated parameter was the steady-state volume of distribution (Vdss), which reflects the extent to which a drug is distributed into tissues relative to plasma (Abdurrahman et al., 2021). Compounds with Vdss values below 1.41 are considered to have low distribution, whereas values above 2.82 indicate high tissue distribution. The analysis showed that minoxidil and tomatine have Vdss values of 1.39 and 0.258, while isorhamnetin displayed a higher log Vdss of 13.28, indicating better tissue distribution compared to minoxidil and tomatine (Table VI).

Drug metabolism primarily takes place in the liver and involves cytochrome P450 (CYP) enzymes (Deviana & Diniatik, 2021). CYP2C9 plays a role in regulating the metabolism of various drugs, whereas CYP3A4 facilitates biotransformation through reactions such as oxidation, hydroxylation, and dealkylation to enhance drug elimination. Inhibition of these enzymes may alter drug metabolism and influence therapeutic efficacy (Febri et al., 2023; Sifaiya et al., 2024).

The metabolic prediction results presented in Table VII indicate that the test ligand is neither a substrate of the CYP3A4 enzyme nor an inhibitor of CYP2C9, suggesting a low likelihood of metabolic interactions. The estimated total clearance parameter showed that the compound exhibits a relatively slow excretion rate (Table VIII), which may reduce the risk of toxicity, as compounds with high molecular weight and hydrophobicity are often eliminated less efficiently (Krihariyani et al., 2020). Furthermore, AMES toxicity prediction revealed that the test ligand did not exhibit mutagenic effects, indicating a favorable safety profile (Table IX).

## IV. CONCLUSION

Docking analysis revealed that isorhamnetin exhibited a stronger binding affinity (−8.398 kcal/mol) than the reference ligand minoxidil (−7.353 kcal/mol). Supported by favorable ADME-Tox properties, particularly in skin permeability, absorption, and distribution, isorhamnetin shows promise as an androgen receptor antagonist for alopecia therapy.

## CONFLICT OF INTEREST

The authors declare no conflict of interest.

## ACKNOWLEDGEMENT

This research was supported by the Basic Research scheme Grant of DIPA Faculty of Medicine Universitas Lampung number:1396/UN26.18/PN.01/2025. The authors would like to extend their high appreciation to the Rector through the Research Institution and Community Service, and the Dean Faculty of Medicine, Universitas Lampung.

## REFERENCES

Abdurrahman, S., Ruslin, R., Hasanah, A., & Mustarichie, R. (2021). Molecular docking studies and ADME-Tox prediction of phytocompounds from Merremia peltata as a potential anti-alopecia treatment. *Journal of Advanced Pharmaceutical Technology and Research*, *12*(2), 132–139. https://doi.org/10.4103/japtr.JAPTR_222_20

Abdurrahman, S., Ruslin, R., Hasanah, A. N., Mustarichie, R., & Ifaya, M. (2022). Active Antialopecia Chemical Identification of Merremia peltata Leaves and Computational Study toward Androgen Receptor Using Molecular Docking and Molecular Dynamic Simulation. *Scientific World Journal*, *2022*, 1123047. https://doi.org/10.1155/2022/1123047

Badolati, N., E. Sommella, G. Riccio et al. (2018). Annurca apple polyphenols ignite keratin production in hair follicles by inhibiting the pentose phosphate pathway and amino acid oxidation. *Nutrients*, *10*(10),1406. https://doi.org/10.3390/nu10101406

Cahyaningrum, L., Rubianti, R., Mahira, T., Gabriel, K., Rusdin, A., & Novitasari, D. (2024). in silico study of secondary metabolites in tahongai plant (*Kleinhovia hospita* L.) As a candidatefor hepatocelluler carcinoma therapeutic agent targeting c-met receptor). *Indonesian Journal of Pure and Applied Chemistry*, *7*(2), 83–93. https://doi.org/10.26418/indonesian.v7i2.82567

Chinelo, O. J., Innocent, O. S., Ugochukwu, O. C., & Uzoka, Ijeoma S. (2018). Comparison Of Anti-Dandruff Activity Of Synthetic Shampoos And Crude Plant Extracts On Dandruff Causing Isolates. *IOSR Journal of Biotechnology and Biochemistry (IOSR-JBB*, *4*(3), 42–46. https://doi.org/10.9790/264X-0403014246

Deviana, K. Z., Diniatik, D. (2021). Analisis Penambatan Molekuler dan Prediksi Toksisitas dan ADME Penghambat Enzim Dipeptidil Peptidase IV dari Senyawa Aktif Momordica charantia L. sebagai Antidiabetes. *Pharmaceutical Journal of Indonesia, 18*(2), 361-370. https://doi.org/10.30595/pharmacy.v18i2.8556

Febri, F. A., Chilfi, T., Salamah, A. F., Wilipangga, A. (2023). Analisis Farmakokinetik Dan Toksisitas Pada Kandungan Fenolik Ekstrak Daun Salam (*Syzygium polyanthum*) Menggunakan In Silico pkCMS Dan Protox II. *J Bina Cipta Husada, 1*9(1), 108–117. https://jurnal.stikesbch.ac.id/index.php/jurnal/article/view/95

Guo, E. L., & Katta, R. (2017). Diet and hair loss: effects of nutrient deficiency and supplement use.

*Dermatology Practical & Conceptual*, *7*(1), 1–10. https://doi.org/10.5826/dpc.0701a01

Krihariyani, D., Sasongkowati, R., & Haryanto, E. (2020). Studi In Silico Sifat Farmakokinetik, Toksisitas, Dan Aktivitas Imunomodulator Brazilein Kayu Secang Terhadap Enzim 3 Chymotrypsin-Like Cysteine Protease Coronavirus. *Journal of Indonesian Medical Laboratory and Science*, *1*(1), 76–90. https://doi.org/10.53699/joimedlabs.v1i1.14

Mardianingrum, R., Bachtiar, K. R., Susanti, S., Aas Nuraisah, A. N., & Ruswanto, R. (2021). Studi In Silico Senyawa 1,4-Naphthalenedione-2-Ethyl-3-Hydroxy sebagai Antiinflamasi dan Antikanker Payudara. *ALCHEMY Jurnal Penelitian Kimia*, *17*(1), 83. https://doi.org/10.20961/alchemy.17.1.43979.83-95

Mustarichie, R., & Hasanah, A. N. (2019). Anti-alopecia activity of waste cacao (Theobroma cacao L.) peels. *Drug Invention Today*, *11*(9), 2194-2199.

Mustarichie, R., Megantara, S., & Saptarini, N. M. (2017). In-silico study of bioactive compounds of natural materials as a JAK-signal transducer and activator of transcription inhibitor for anti-alopecia. *Asian Journal of Pharmaceutical and Clinical Research*, *10*(11), 331–336. https://doi.org/10.22159/ajpcr.2017.v10i11.21118

Mustarichie, R., Wicaksono, I. A., & Gozali, D. (2017). Anti-alopecia activity of DADAP (Erythrina variegata L.) leaves ethanol extract. *Journal of Pharmaceutical Sciences and Research, 9*(10), 1849-1854. https://api.semanticscholar.org/CorpusID:212594042

Mustarichie, R., Wicaksono, I. A., & Hayati, C. (2018). Anti-Alopecia Characteristics of Ethanol Extract, n-Hexane, Ethyl acetate and Water Fractions of Malvaviscus arboreus Cav. *Research Journal of Pharmacy and Technology*, *11*(11), 5066–5072. https://doi.org/10.5958/0974-360X.2018.00924.1

Oktoba, Z., Moektiwardoyo, M., & Mustarichie, R. (2018). In vivo hair growth stimulating activity of ethanol extract and its fractions from rampai lampung (*Lycopersicon esculentum* Mill.) Leaves. *International Research Journal Of Pharmacy*, *9*(9), 87–92. https://doi.org/10.7897/2230-8407.099193

Oktoba, Z., Moektiwardoyo, M., & Mustarichie, R. (2019). Active Compound From N-Hexane Fraction Of Rampai (*Lycopersicon esculentum*) Leaves Ethanol Extract. *International Journal of Pharmaceutical Sciences and Research*, *10*(5), 2537. https://doi.org/10.13040/IJPSR.0975-8232.10(5).2537-44

Pantsar, T., & Poso, A. (2018). Binding affinity via docking: Fact and fiction. *Molecules, 23*(8), 1899. https://doi.org/10.3390/molecules23081899

*RCSB PDB - 4K7A: Crystal structure of the androgen receptor ligand binding domain in complex with minoxidil*. Retrieved December 27, 2025, from https://www.rcsb.org/structure/4K7A

Shofi, M. (2021). Uji in silico aktivitas sitotoksik dan toksisitas senyawa bioaktif biji trembesi (*Samanea saman* (jacq.) Merr) sebagai kandidat obat diabetes mellitus. Jurnal Pharma Bhakta, *1*(2), 1-14. https://jurnalpharmabhakta.iik.ac.id/index.php/jpb/article/view/10

Sifaiya, L., Hasan, R., Choirunniza, A., N. (2024). Kajian molekular docking, farmakokinetik dan toksisitas

tanaman pegagan (*Centella asiatica* L.) terhadap target terapi antidepresan. *Pharmasipha Pharm J Islam Pharm*, *8*(2), 26–40. https://doi.org/10.21111/pharmasipha.v8i2.11772

Weni, M., Safithri, M., & Seno, D. S. H. (2020). Molecular docking of active compounds Piper crocatum on the a-glucosidase enzyme as antidiabetic. *Indonesian Journal of Pharmaceutical Science and Technology,* *7*(2), 64-72. https://doi.org/10.24198/ijpst.v7i2.21120